Applied Catalysis B: Environmental 237 (2018) 302–308

Contents lists available at ScienceDirect

Applied Catalysis B: Environmental

journal homepage: www.elsevier.com/locate/apcatb

Bi quantum dots obtained via in situ photodeposition method as a new photocatalytic CO_2 reduction cocatalyst instead of noble metals: Borrowing redox conversion between Bi_2O_3 and Bi

Guihua Yang[a], Wenkang Miao[a], Zhimin Yuan[a], Zaiyong Jiang[a,*], Baibiao Huang[b,*], Peng Wang[b], Jiachuan Chen[a]

[a] State Key Laboratory of Biobased Material and Green Papermaking, Qilu University of Technology, Shandong Academy of Sciences, Jinan 250353, PR China
[b] State key Laboratory of Crystal Materials, Shandong University, Jinan 250100, PR China

ARTICLE INFO

Keywords:
Metal Bi
Cocatalysts
Photocatalytic CO_2reduction
Quantum dots

ABSTRACT

Metal Bi is applied as the cocatalyst instead of noble metals, for the first time, in photocatalytic CO_2 reduction and exhibits significant increase in CO yield compared to that of pristine photocatalyst, about 4.8 times. In situ photodeposition method is used to prepare metal Bi. Surprisingly, the average size of metal Bi obtained is ca. 5 nm and can be considered as quantum dots level, which is very difficult to be realized for noble metals via in situ photodeposition. Unfortunately, such small Bi is unstable in air, making it very difficult for the preservation. Another fortunate phenomenon is discovered, the unstable metal Bi can be stored via using the form of Bi/Bi_2O_3 quantum dots (Bi_2O_3 is main body of white Bi/Bi_2O_3 composites). When carried out the photocatalytic CO_2 reduction, the white Bi/Bi_2O_3 can be easily transformed into grey Bi/Bi_2O_3 composites (the main body of grey Bi/Bi_2O_3 composites is metal Bi) to improve the photocatalytic CO_2 reduction rate. This reason is that CB level of Bi_2O_3 quantum dots has shifted to a more negative position due to quantum confinement effect compared to the standard redox potential of Bi_2O_3/Bi (0.37 eV), leading to Bi_2O_3 easily to be reduced to metal Bi under the effect of photogenerated electrons derived from TiO_2. This work demonstrated the mutual conversion between storage and utilization may offer an attractive approach for the application of unstable quantum dot materials or single atom materials.

1. Introduction

Since the first report about photocatalytic reduction of CO_2 to chemical fuels by Halmann in 1978 [1], semiconductor photocatalysts have be used extensively in relieving the deficiency of energy and the environmental problems of the greenhouse gas, CO_2 [2–5]. Up to now, the researchers have discovered many kinds of semiconductor photocatalysts for the reduction of CO_2. For example, TiO_2 [6], $BiVO_4$ [7], ZnS [8], Bi_2WO_6 [9], CdS [10], $SrTiO_3$ [11], and $ZnIn_2S_4$ [12], etc have been widely applied to drive the CO_2 conversion under solar irradiation. Generally speaking, there are three main limited factors in the whole photocatalytic CO_2 reduction process [13]: 1) the semiconductors need absorb sufficient solar light to produce more electron and hole pairs, 2) suppress the recombination of photo-generated electron and hole pairs and transfer more electron to the surface of photocatalysts for CO_2 reduction, 3) surface photocatalytic reaction for water oxidation and the reduction of CO_2. In the past few decades, much work has been focused on the first two processes to extend the light absorption range of photocatalysts and promote the separation efficiency of photo-generated electrons and holes of semiconductors. And these explorations of photocatalytic CO_2 reduction activity have achieved many remarkable results. However, there are seldom reports about the third processes to improve the CO_2 photo-conversion activity [13]. Therefore, further exploration is very valuable for both scientific research and practical applications. As far as we know, the third process could be enhanced via depositing electron and/or hole cocatalysts on surface of photocatalysts [13], which has many significant effects on whole photocatalytic CO_2 reduction reaction. For instance, they can trap electron or hole to facilitate charge carrier separation, improve the photocatalytic performance and selectivity of products, increase stability of photocatalysts, restrain the side or back reactions, and so on.

Currently, the studies of cocatalysts are main focused on noble metal-based materials, such as Pt, Ag, Au, Pd, Ru, and so on have been widely used as high active and selective cocatalysts in the process of photcatalytic CO_2 reduction [14–18]. Although noble metal-based cocatalysts have obtained many remarkable achievements, it is difficult

* Corresponding authors.
E-mail addresses: zaiyongjiang@qlu.edu.cn (Z. Jiang), bbhuang@sdu.edu.cn (B. Huang).

https://doi.org/10.1016/j.apcatb.2018.06.018
Received 2 April 2018; Received in revised form 17 May 2018; Accepted 4 June 2018
Available online 04 June 2018

for their industrial-scale applications due to the low storage and high price. Therefore, the exploration of noble metal-free cocatalysts becomes a tendency and attracts more and more attention. For example, Wang et al. prepared the cobalt-containing zeolitic imidazolate framework using as a cocatalyst and exhibiting an obvious improvement of yield of CO [19]. Chen et al. prepared Cu/GO (graphene oxide) hybrids, in which the metallic copper nanoparticles were uniformly deposited on the surface of GO and the introduction of Cu has remarkable enhanced the CO_2 photoconversion performance of GO via suppressing the recombination of electron and hole pairs [20]. Ye et al. realized single Co atoms incorporation into MOF matrix, which greatly boost the electron and hole separation efficiency, leading to significantly enhanced photocatalytic CO_2 reduction activity [21]. Up to now, there are only few kinds of noble metal-free cocatalysts to have been found, mainly including Cu, Ni/NiO, Co-incorporated metal organic framework (MOF) and nano-carbons. Therefore, further explorations on new cocatalysts with high photocatalytic CO_2 reduction activity, selectivity and low cost are of great importance for both scientific research and practical applications.

Very recently, high earth abundance and inexpensive Bi (bismuth) has been considered as a promising candidate for noble metal cocatalysts, which has been coupled with some semiconductors via using typical solvothermal method, such as, $(BiO)_2CO_3$, C_3N_4, BiOI, $ZnWO_4$ [22–25]. In which Bi was used as cocatalysts to accelerate the charge carrier separation, thus obtained excellent photocatalytic activity over the degradation of organic dyes and NO gas. Up to now, there is no a report whether the Bi can been used as the cocatalyst of photocatalytic CO_2 reduction. Therefore, systematic research is very necessary and great importance. Moreover, we all know that coupling noble metal cocatalysts with photocatalysts mainly adopted simple in situ photodeposition method and if the size of cocatalysts is smaller, especially ultrathin layer or quantum dots (which can provide more active sites) [9], the performance of CO_2 photoconversion will be much better. However, current studied Bi cocatalyst was main obtained via typical solvothermal method, which has a complex operational process and is easy to make secondary pollution compared with the in situ photodeposition method. And the investigated size is generally in 10–200 nm. So, we decided to try to use the in situ photodeposition method to couple metal Bi with photocatalysts, simultaneously control process to obtain Bi quantum dots, then used as cocatalyst of photocatalytic CO_2 reduction. The exploration is of great important for both scientific research and practical applications.

In this paper, we have realized the preparation of Bi quantum dots via in situ photodeposition method for the first time, which uniformly disperse on the surface of TiO_2 and firstly used it as the cocatalyst of CO_2 photoconversion and achieved remarkably improved CO_2 photoconversion activity compared to that of pristine photocatalyst. During and after phtocatalytic CO_2 reduction, Bi/Bi_2O_3 exhibits two different forms of existence, respectively. These two forms can be mutually transformed under UV–vis light irradiation, realizing the cycle between storage and utilization of metal Bi cocatalyst.

2. Experimental

2.1. Materials

Tetrabutyl titanate, 40% HF solution and $Bi(NO_3)_3{\cdot}5H_2O$ were provided from the Sinopharm Chemical Reagent Corporation (Shanghai, China). All experimental materials, which were used without further purification, were analytical grade in this study.

2.2. Synthesis of TiO_2 and $TiO_2/Bi/Bi_2O_3$ composite photocatalysts

The TiO_2 *nanosheets* was synthesized according to the literature reported by Prof Yu [26]. The process of preparation was as follows: HF (3 mL) was added into 25 ml of tetrabutyl titanate, the mixed suspension solution was continually stirred for 10 min. Subsequently, the resulting precursor suspension was kept in a 100 mL autoclave, which is maintained at 200 °C for 24 h. The autoclave was allowed to cool to room temperature, the as-prepared sample was washed via deionized water and absolute ethanol, respectively. The obtained product was dried at 60 °C for 6 h in an oven.

A series of $TiO_2/Bi/Bi_2O_3$ composite photocatalysts was prepared via an in situ photodeposition method with different $Bi(NO_3)_3{\cdot}5H_2O$ amount (including 0.1 g TiO_2, 3 mg, 6 mg, 12 mg, 18 mg $Bi(NO_3)_3{\cdot}5H_2O$ and 100 ml deionized water) in CO_2 atmosphere with controlling the temperature at 15 °C using cooling water circulation. The illumination time is 4 h, the corresponding products were noted as $TiO_2/Bi/Bi_2O_3$-1, $TiO_2/Bi/Bi_2O_3$-2, $TiO_2/Bi/Bi_2O_3$-3 and $TiO_2/Bi/Bi_2O_3$-4. After illumination treatment, the resulting solution was filtrated and washed using deionized water for three times. After that, the obtained $TiO_2/Bi/Bi_2O_3$ was dried at 60 °C in an oven.

2.3. Characterization

The all products were analyzed by using X-ray powder diffraction (XRD) on a Bruker AXS D8 advance powder diffractometer with Cu KαX-ray radiation. The particle sizes and morphologies of the samples were analyzed via using a Hitachi S-4800 microscope with an accelerating voltage of 7.0 kV. Transmission electron microscope (TEM) and high-resolution transmission electron microscopy (HRTEM) measurements were performed by a JEOL-2100 microscope. The UV–vis diffuse reflectance spectra were carried out on a Shimadzu UV 2550 recording spectrophotometer, which is equipped with an integrating sphere with $BaSO_4$ as a reference. Fluorescence spectra were measured under 320 nm excitation. X-ray photoelectron spectroscopy (XPS) was performed using a Thermo Fisher Scientific (ESCALAB 250) X-ray photoelectron spectrometer and the result was charge corrected to the adventitious C 1 s peak at 284.6 eV.

2.4. Photocatalytic CO_2 reduction evaluation

The process of CO_2 photoconversion is as follows: The sample (0.1 g) was dispersed into 100 mL water with vigorous stirring and continuously bubbled using high purity CO_2 gas for 15 min A 300 W Xe arc lamp (PLS-SXE300, Beijing Trusttech Co., Ltd.) was applied as the light source and the temperature of reactor of CO_2 photoconversion was kept at 15° via using cooling water circulation equipment. At the given time interval, the gas was got out and monitored via Varian CP-3800 gas chromatograph (FID detector, Propark Q column).

3. Results and discussion

We choose the TiO_2 nanosheets as the semiconductor substrate. Firstly, we directly adopt in situ photodeposition method according to the approach of noble metal cocatalysts (Pt, Ag, Pd, Au) in air. We have not observed any change, the mixed solution was still colourless (Fig. S1), which indicates metal Bi has no generated. Considering that metal Bi produced under light irradiation may be very unstable in air, simultaneously supervise whether the as-prepared product has excellent performance of CO_2 photoconversion, we directly carried out the in situ photodeposition in CO_2 atmosphere with controlling the temperature at 15 °C using cooling water circulation. Fortunately, we found that the colourless suspension solution became gray under light irradiation (Fig. S2) and a lot of CO (carbon monoxide) was detected, indicating the metal Bi may be formed and exhibit excellent CO_2 photoconversion activity. Subsequently, the concentration of bismuth nitrate was optimized via detecting the yield of CO (Fig. 1a), a series of as-prepared samples were prepared and noted as $TiO_2/Bi/Bi_2O_3$-1, $TiO_2/Bi/Bi_2O_3$-2, $TiO_2/Bi/Bi_2O_3$-3, and $TiO_2/Bi/Bi_2O_3$-4 based on different amounts of Bi $(NO_3)_3$ $5H_2O$. It is observed that the CO_2 photoreduction activities for $TiO_2/Bi/Bi_2O_3$ samples are significantly improved compared to pristine

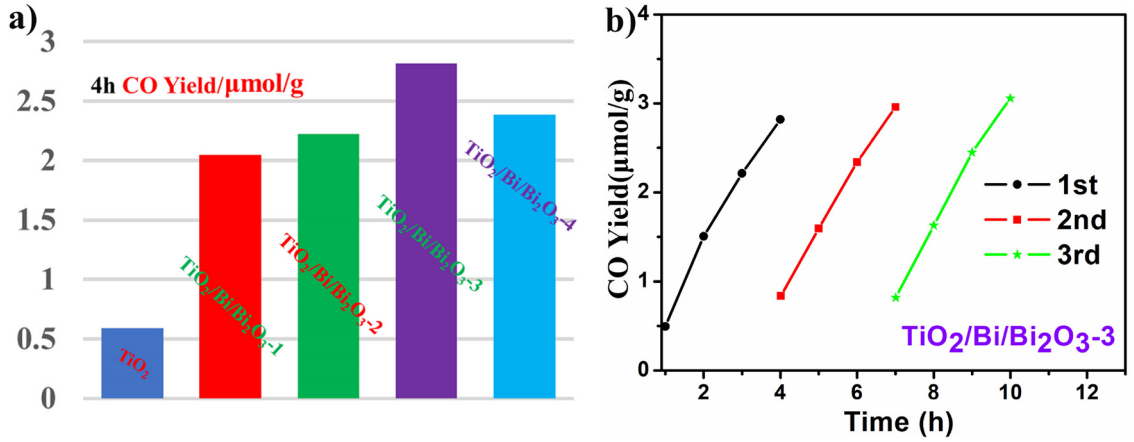

Fig. 1. (a) CO yield during the optimization process of the concentration of bismuth nitrate under UV–vis light irradiation. (b) Repeated photocatalytic CO_2 reduction activity in H_2O without bismuth nitrate over white TiO_2/Bi/Bi_2O_3-3 sample for as photocatalyst for two times (2nd and 3rd).

TiO_2. Among them, the TiO_2/Bi/Bi_2O_3-3 has exhibited the highest activity of CO_2 photoconversion, in which the relative reaction rate is about 4.8 times higher than that of pristine TiO_2.

However, when the reactor is opened to obtain the as-prepared samples, a new problem occurred. Suddenly the grey suspension solution becomes colorless (Fig. S3), indicating the high active and unstable metal Bi may have been oxidized in air. Subsequently, the colourless suspension solutions were filtrated and washed several times with deionized water, which was dried in an oven at 60 °C for 6 h. In order to confirm whether the new obtained TiO_2/Bi/Bi_2O_3 samples can still keep the excellent CO_2 reduction activity, the photocatalytic CO_2 reduction reaction of TiO_2/Bi/Bi_2O_3-3 was circularly carried out for two times in water solution. As shown in Fig. 1b, the new obtained TiO_2/Bi/Bi_2O_3-3 displays similar photocatalytic CO_2 activity with above result. Surprisingly, the colourless suspension solution without bismuth nitrate also became the grey (Fig. S4), again. After finishing the photocatalytic CO_2 reduction, the reactor is opened with stirring for several minutes, subsequently, the gray suspension solution transformed colourless. Subsequently, the second cyclic sample was filtrated and dried in oven at 60 °C for 6 h, noting as "2sample". And then, the 2 sample was continued to perform photocatalytic CO_2 conversion in water solution, again. The result is the similar to the second cycle (Fig. S5). The results imply that TiO_2/Bi/Bi_2O_3-3 photocatalyst has carried out a relatively stable cyclic reaction under ultraviolet visible (UV–vis) light irradiation.

In order to systematically investigate the result, the crystalline structures of the as-prepared samples were firstly characterized via using powder X-ray diffraction (XRD). As can be seen in Fig. 2a, these diffraction peaks for all samples can be perfectly identified as the anatase TiO_2 structure (JCPDS no. 21-1272). Moreover, a slightly weak peak ascribed to cubic metal Bi (JCPDS no. 26-214) was observed in the XRD patterns of TiO_2/Bi/Bi_2O_3 samples and the intensity gradually increased with the enhancement of content of metal Bi, indicating the presence of metal Bi in the as-prepared samples. There are no diffraction peaks of Bi_2O_3 in the TiO_2/Bi/Bi_2O_3 samples, which suggests the Bi_2O_3 producted via the oxidation of metal Bi is amorphous.

To identify the valence states of the Bi ions and the chemical composition of the deposited samples, TiO_2/Bi/Bi_2O_3-3 sample chosen as an example was analyzed through XPS. For comparison, pristine TiO_2 sample was also investigated. And the high resolution XPS spectra of the Bi 4f (Fig. 2b), O1s (Fig. 2c) and Ti 2p (Fig. 2d) binding energy regions are shown in Fig. 2. As shown in Fig. 2b, the XPS peak of Bi ions can be decomposed into four Gaussian peaks, two strong peaks locations at 164.3 and 158.9 eV in TiO_2/Bi/Bi_2O_3-3 sample, which can be attributed to the characteristic orbital splitting of the Bi $4f_{5/2}$ and Bi $4f_{7/2}$ and are features of the Bi^{3+}. Also, two low peaks centered at 162.1 and 156.9 eV can be ascribed to metallic Bi^0 species.[24] Furthermore, there are two similar peaks centered at 530.0 and 532.9 eV in both samples (Fig. 2c), which are assigned to the lattice oxygen and hydroxyl groups adsorbed onto the surface of samples. Furthermore, an additional small peak was presented in the XPS spectrum of O1 s, which is correspond to oxygen vacancies. The oxygen vacancies is likely to derive from amorphous Bi_2O_3 due to the incomplete oxidation of Bi quantum dots. The results further proved both metal Bi and Bi_2O_3 are co-existence in the TiO_2/Bi/Bi_2O_3 samples. Fig. 2d showed the similar binding energies of Ti^{4+} are 458.8 and 464.5 eV, respectively, in both samples. However, there are no peaks of Ti^{3+} observed in the XPS spectra. The result suggests the introduction of Bi/Bi_2O_3 has no lead to structural change of TiO_2 and there is no chemical bond to be formed between Ti atom and Bi atom.

The morphologies of pure TiO_2 and TiO_2/Bi/Bi_2O_3 samples were investigated via scanning electron microscopy (SEM). As shown in Figs. S6 and S7, the morphologies are almost identical after the deposition of Bi/Bi_2O_3. And then, Fig. S8 exhibits the energy-dispersive X-ray spectrum (EDS) information of the TiO_2/Bi/Bi_2O_3, further confirming the presence of Bi elements and getting relative molar ratios of Bi elements in TiO_2/Bi/Bi_2O_3 samples for 0.49% (TiO_2/Bi/Bi_2O_3-1), 1.46% (TiO_2/Bi/Bi_2O_3-2), 3.67% (TiO_2/Bi/Bi_2O_3-3), 5.12% (TiO_2/Bi/Bi_2O_3-4), respectively. As so to further analyze the surface morphologies of samples, TiO_2/Bi/Bi_2O_3-3 was chosen as an example and the surface state was investigated using the transmission electron microscope (TEM). For comparison, pristine TiO_2 was also characterized. It is observed that the average sides of TiO_2 nanosheets are about 30 nm (width) and 50 nm (length), respectively (Fig. 3a). The insert image of Fig. 3b showed the measured lattice spacing is ca. 0.351 nm, which is matched with the (101) planes of pristine anatase TiO_2. After the deposition of Bi/Bi_2O_3, the sizes of TiO_2 nanosheets have no obvious change (Fig. 3c and d) and the Bi/Bi_2O_3 nanoparticles uniformly disperse on the TiO_2 nanosheets, in which their average particle size is quantum dots level, ca. 5 nm. Moreover, for a closer and careful observation via the TEM, we found the lattice fringes of many quantum dots quickly and continually change under the electron beam irradiation of TEM, which may be due to the high active and instability of quantum dots except their own natural defects of Bi-based materials. A catched lattice spacing is ca. 0.3096 nm, which can be assigned to the (001) crystal plane of metal Bi (Fig. 3d). In addition, to check whether the Bi/Bi_2O_3 quantum dots can still steadily immobilized on the surface of TiO_2 nanosheets after photocatalytic CO_2 reduction, we have characterized the TEM of TiO_2/Bi/Bi_2O_3-3 sample subjected to three consecutive photocatalytic experiments (Fig. S9). Compared with the initial TiO_2/Bi/Bi_2O_3-3 TEM patterns, there is no change after three cycles, indicating that TiO_2/Bi/Bi_2O_3-3 is very stable and really have industrial application prospects.

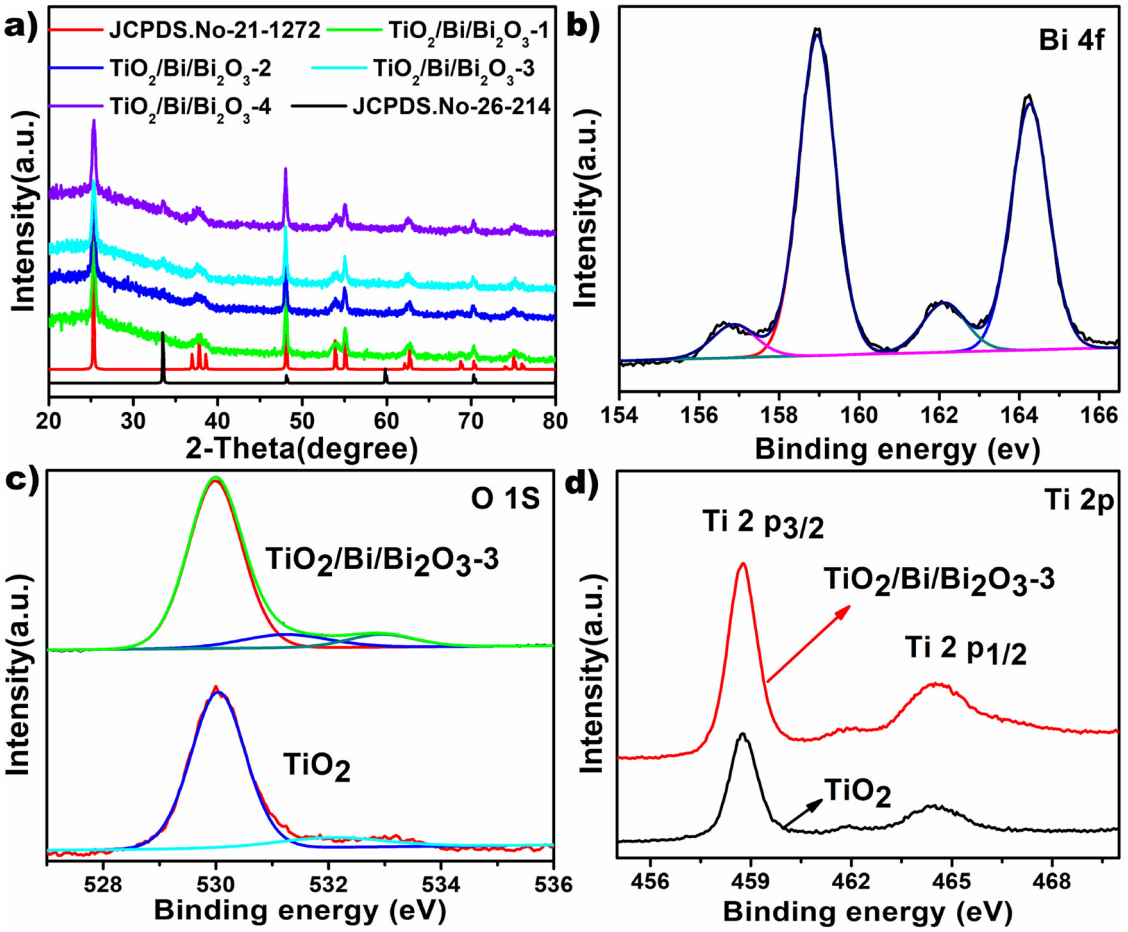

Fig. 2. (a) XRD patterns of all samples, High-resolution XPS spectra of TiO_2/Bi/Bi_2O_3-3 and pristine TiO_2 samples: (b) Bi 4f, (c) O 1 s and (d) Ti 2p.

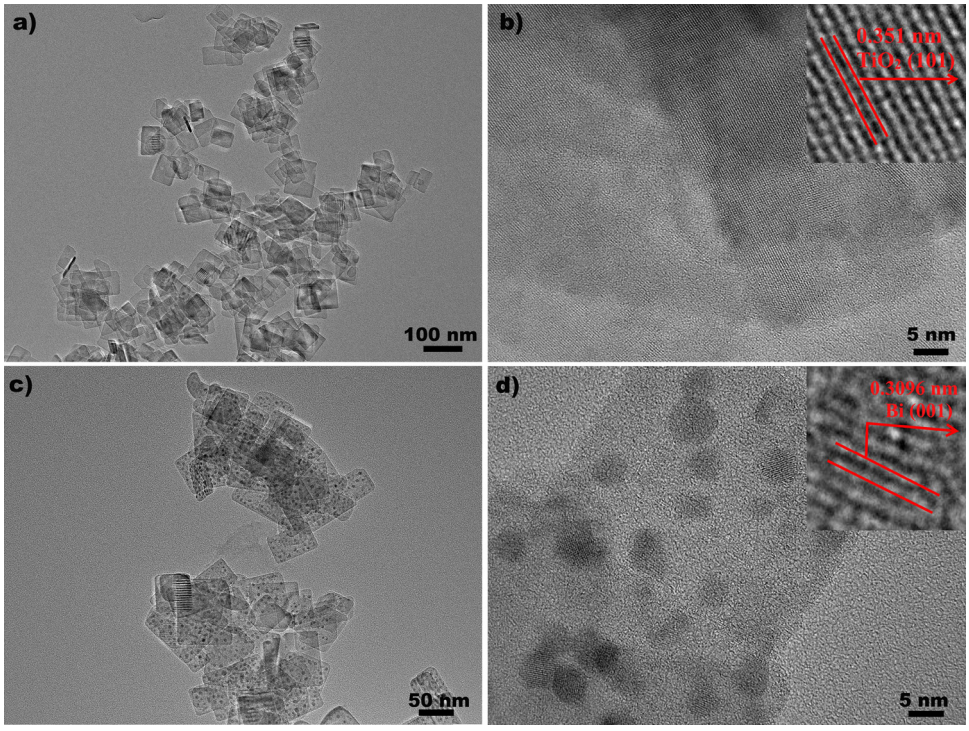

Fig. 3. TEM images of TiO_2 (a, b) and TiO_2/Bi/Bi_2O_3-3 (c, d).

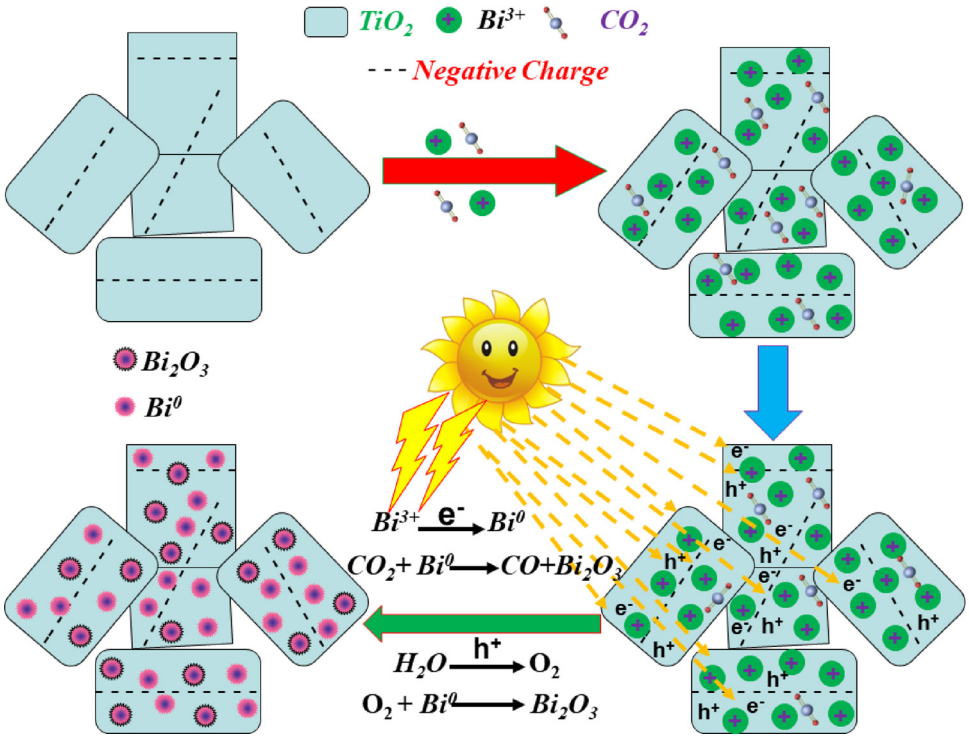

Fig. 4. Schematic representation of the photodeposition process of Bi/Bi_2O_3 quantum dots on the surface of TiO_2 nanosheets.

In order to explore the deposition mechanism of Bi/Bi_2O_3 quantum dots on the surface of TiO_2 nanosheets, the zeta potential of TiO_2 nanosheets was measured. The value is -2.12, which is electronegative. Based on the above investigation, a possible in situ photodeposition mechanism of $TiO_2/Bi/Bi_2O_3$ composites was proposed as illustrated in Fig. 4. Due to the electrostatic interactions, the Bi^{3+} with positive charges could be easily absorbed on the surface of TiO_2 nanosheets with negative charges. Under UV–vis light irradiation, the photo-generated electrons on conduction band (CB) of TiO_2 transfer to its surface, and react with Bi^{3+} adsorbed on the surface of TiO_2 nanosheets, thereby forming Bi° under the protection of CO_2 gas, or else Bi^0 will be oxidized immediately by oxygen in H_2O or air. And, the some Bi^0 reduces the CO_2 to CO and generates Bi_2O_3. In the other hand, the photo-generated holes on valence band (VB) transfer to the surface of TiO_2 and react with adsorbed water to form O_2, partial oxygen may participate in the oxidation of Bi^0. Therefore, the grey $TiO_2/Bi/Bi_2O_3$ composites were successfully obtained and the Bi^0 is main body in Bi/Bi_2O_3 composite. But, after the reactor is opened, Bi_2O_3 is main body in the white $TiO_2/Bi/Bi_2O_3$ composites obtained via filtration.

Fig. 5a illustrates the UV–vis absorption spectra of the pristine TiO_2 and the $TiO_2/Bi/Bi_2O_3$ composites. It could be observed that the absorption edges of $TiO_2/Bi/Bi_2O_3$ are similar compared to that of pristine TiO_2 sample, except a slight red shift on the absorption onset. The result indicates that Bi/Bi_2O_3 composites only contain a small amount of metal Bi. In other words, the main body of white Bi/Bi_2O_3 quantum dots should be Bi_2O_3 rather than metal Bi, or else there will be a very obvious visible light absorption due to the surface plasmon resonance of metal Bi.[23] But, when $TiO_2/Bi/Bi_2O_3$ composites were carried out the phtocatalytic CO_2 reduction, they will exhibit wider light absorption (Figs. S4a and S5a) due to the produce of grey $TiO_2/Bi/Bi_2O_3$ composites(G-TBB) with main body as Bi^0, which derived from the conversion of white $TiO_2/Bi/Bi_2O_3$ composites (W-TBB) with main body as Bi_2O_3. The result indicates that the cocatalyst of metal Bi prepared by us was kept in air via using the form of W-TBB due to the instability of Bi^0, subsequently, W-TBB was transformed into G-TBB during the process of photocatalytic CO_2 reduction. The most attractive point is the mutual transformation between W-TBB and G-TBB in the during and after phtocatalytic CO_2 reduction.

Photoluminescence (PL) spectra were performed to test the recombination rate of photogenerated electrons and holes. As was shown in Fig. 5b, the positions of the emission peaks of $TiO_2/Bi/Bi_2O_3$ were similar compared with that of TiO_2, but all intensity decreased and $TiO_2/Bi/Bi_2O_3$-3 has exhibited the lowest intensity. This result suggests that $TiO_2/Bi/Bi_2O_3$-3 possesses the lowest recombination rate of photogenerated charge carriers compared with pristine TiO_2 and other $TiO_2/Bi/Bi_2O_3$ composites [27–29]. That is to say, the slower recombination rate implies the photogenerated electrons and holes in the $TiO_2/Bi/Bi_2O_3$ composites could be better separated than those in the pristine TiO_2 due to the introductions of Bi/Bi_2O_3 nanoparticles, which has significantly suppressed the recombination of photo-generated charge carriers. This result is consistent with that $TiO_2/Bi/Bi_2O_3$ composites have exhibited much higher photocatalytic CO_2 reduction performance.

Based on the experimental consequences, a possible mechanism for the photocatalytic CO_2 reaction is proposed in Fig. 5c. Under UV–vis light irradiation, TiO_2 is also excited to produce the photogenerated electrons (e^-) and holes (h^+). The electron transfers to the Bi_2O_3 quantum dots immobilized on the surface of TiO_2, leaving a hole in the VB. It is reported that the standard redox potential of Bi_2O_3/Bi is 0.37 eV and the position of CB and VB of bulk Bi_2O_3 is 0.33 and 3.13 eV, respectively [30,31]. Based on the quantum confinement effect, CB level of Bi_2O_3 quantum dots should shift to a more negative position. Therefore, Bi_2O_3 quantum dots will be reduced to Bi^0 quantum dots by the photogenerated electrons derived from TiO_2. The Bi^0 reduces the CO_2 to CO and generates Bi_2O_3. In the other hand, the photo-generated holes flow to the surface of TiO_2, which directly oxidize water molecules giving rise to O_2, subsequently, partial oxygen is likely to participate in the oxidation of Bi^0. In this whole process, the Bi is used as the cocatalyst or an electron traps to induce the efficient separation of photogenerated electrons and holes, thereby enhancing photocatalytic CO_2 reduction activity, which is similar behavior to that of noble metals cocatalysts during the process of CO_2 photoconversion.

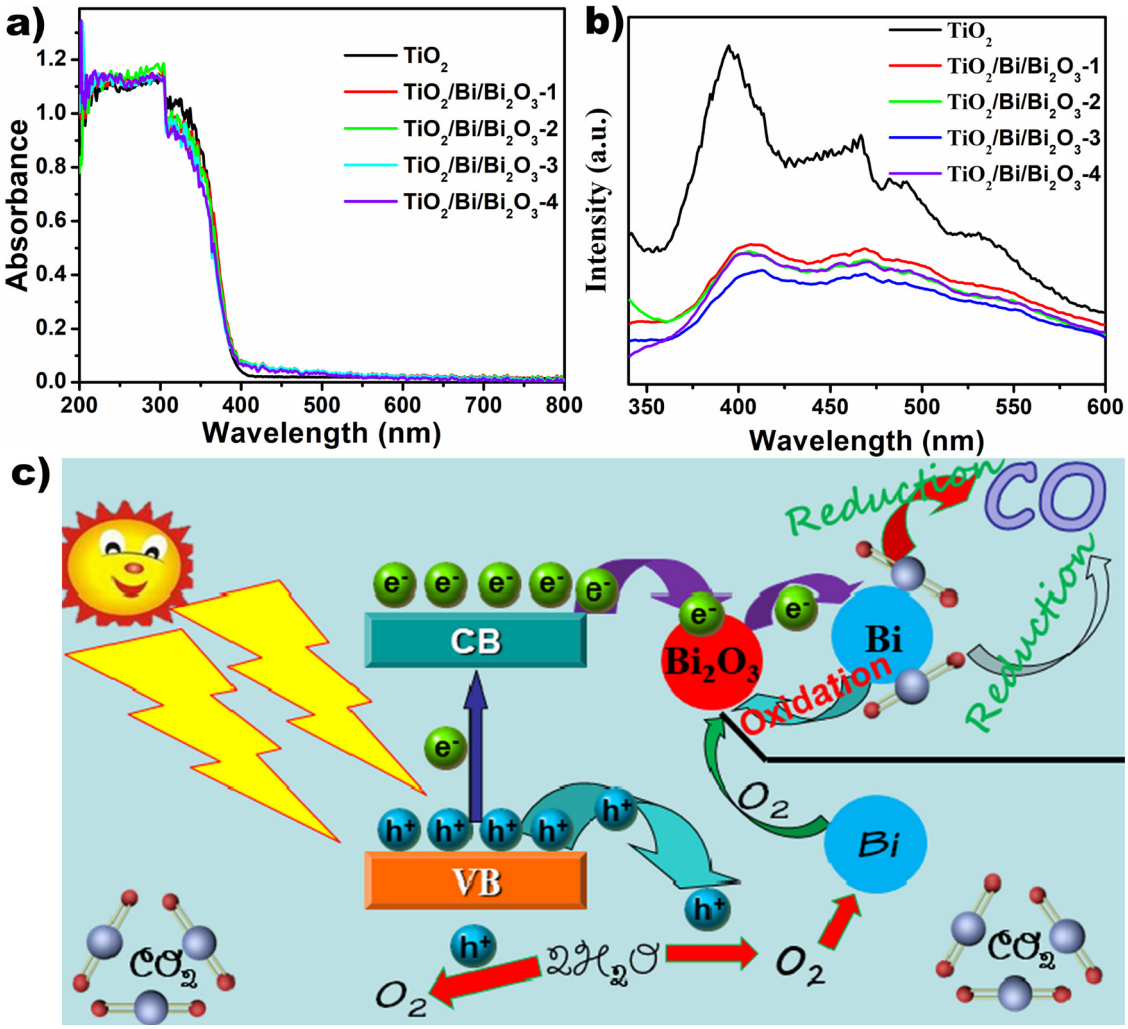

Fig. 5. (a) UV–vis absorption spectra and (b) PL spectra of all samples, (c) The Schematic illustration of photocatalytic CO_2 reduction into CO for $TiO_2/Bi/Bi_2O_3$. (For interpretation of the references to colour in the figure text, the reader is referred to the web version of this article).

4. Conclusions

In summary, we have realized the preparation of Bi/Bi_2O_3 quantum dots via in situ photodeposition method for the first time, which is simple, nontoxic and eco-friendly. The Bi/Bi_2O_3 quantum dots uniformly disperse on the surface of TiO_2 and exhibit two different forms of existence. One is stored form or kept form, Bi_2O_3 is main body of Bi/Bi_2O_3 composites in white $TiO_2/Bi/Bi_2O_3$ kept in air. The other is as cocatalyst or electron traps, Bi° is main body of Bi/Bi_2O_3 composites in grey $TiO_2/Bi/Bi_2O_3$ during the process of phtocatalytic CO_2 reduction, which derived from the conversion of white $TiO_2/Bi/Bi_2O_3$ under UV–vis light irradiation. These two forms can be mutually transformed during and after phtocatalytic CO_2 reduction, leading to the cycle between storage and utilization. In other words, we have sucessfully loaded metal Bi (the noble metal-free cocatalysts) on the surface of semiconductor via in situ photodeposition method, firstly used it as the cocatalyst of CO_2 photoconversion and achieved remarkably improved CO_2 photoconversion activity compared to that of pristine photocatalyst. This work demonstrated the great feasibility of utilizing low-cost Bi nanoparticles as a substitute for noble metals cocatalysts to enhance phtocatalytic CO_2 reduction activity. Using in situ photodeposition method to obtain Bi_2O_3 or Bi quantum dots may open a new avenue for the coupled approach between Bi_2O_3 or Bi nanoparticles with photocatalyst.

Acknowledgments

This work was financially supported by a research Grant from the National Key Research and Development Program of China (Grant No. 2017YFB0307900), the National Natural Science Foundation of China (Grant Nos. 31670595, 31770628), the Taishan Scholars Program, and the Shandong Province Natural Science Foundation (ZR2018BB042).

Appendix A. Supplementary data

Supplementary material related to this article can be found, in the online version, at doi:https://doi.org/10.1016/j.apcatb.2018.06.018.

References

[1] M. Halmann, Nature 275 (1978) 115–116.
[2] G.X. Zhao, W. Zhou, Y.B. Sun, X.K. Wang, H.M. Liu, X.G. Meng, K. Chang, J.H. Ye, Appl. Catal. B: Environ. 226 (2018) 252–257.
[3] X.J. Wang, X.L. Zhao, D.Q. Zhang, G.S. Li, H.X. Li, Appl. Catal. B: Environ. 228 (2018) 47–53.
[4] G.B. Chen, R. Gao, Y.F. Zhao, Z.H. Li, G.I.N. Waterhouse, R. Shi, J.Q. Zhao, M.T. Zhang, L. Shang, G.Y. Sheng, X.P. Zhang, X.D. Wen, L.Z. Wu, C.H. Tung, T.R. Zhang, Adv. Mater. 30 (2018) 1704663.
[5] J. Ding, Y.F. Bu, M. Ou, Y. Yu, Q. Zhong, M.H. Fan, Appl. Catal. B: Environ. 202 (2017) 314–325.
[6] A. Iwase, S. Yoshino, T. Takayama, Y.H. Ng, R. Amal, A. Kudo, J. Am. Chem. Soc. 138 (2016) 10260–10264.
[7] L.Q. Tang, L.B. Kuai, Y.C. Li, H.J. Li, Y. Zhou, Z.G. Zou, Nanotechnology 29

(2018) 6.
[8] Z.Y. Jiang, X.Z. Liang, H.L. Zheng, Y.Y. Liu, Z.Y. Wang, P. Wang, X.Y. Zhang, X.Y. Qin, Y. Dai, M.H. Whangbo, B.B. Huang, Appl. Catal. B: Environ. 219 (2017) 209–215.
[9] L. Liang, F.C. Lei, S. Gao, Y.F. Sun, X.C. Jiao, J. Wu, S. Qamar, Y. Xie, Angew. Chem. Int. Ed. 54 (2015) 13971–13974.
[10] J. Jin, J.G. Yu, D.P. Guo, C. Cui, W.K. Ho, Small 11 (2015) 5262–5271.
[11] Q. Kang, T. Wang, P. Li, L.Q. Liu, K. Chang, M. Li, J.H. Ye, Angew. Chem. Int. Ed. 127 (2015) 855–859.
[12] G. Yang, D.M. Chen, H. Ding, J.J. Feng, J.Z. Zhang, Y.F. Zhu, S. Hamid, D.W. Bahnemann, Appl. Catal. B: Environ. 219 (2017) 611–618.
[13] J.R. Ran, M. Jaroniec, S.Z. Qiao, Adv. Mater. 30 (2018) 1704649.
[14] H. Shi, T. Wang, J. Chen, C. Zhu, J. Ye, Z. Zou, Catal. Lett. 141 (2011) 525–530.
[15] P. Pathak, M.J. Meziani, L. Castillo, Y.-P. Sun, Green Chem. 7 (2005) 667–670.
[16] K.S. Raja, Y.R. Smith, N. Kondamudi, A. Manivannan, M. Misra, V.R. Subramanian, Electrochem. Solid-State Lett. 14 (2011) F5.
[17] W. Kim, T. Seok, W. Choi, Energy Environ. Sci. 5 (2012) 6066–6070.
[18] S.C. Yan, S.X. Ouyang, J. Gao, M. Yang, J.Y. Feng, X.X. Fan, L.J. Wan, Z.S. Li, J.H. Ye, Y. Zhou, Z.G. Zou, Angew. Chem. Int. Ed. 49 (2010) 6400–6404.
[19] S.B. Wang, W.S. Yao, J.L. Lin, Z.X. Ding, X.C. Wang, Angew. Chem. Int. Ed. 53 (2014) 1034–1038.
[20] I. Shown, H.C. Hsu, Y.C. Chang, C.H. Lin, P.K. Roy, A. Ganguly, C.H. Wang, J.K. Chang, C.I. Wu, L.C. Chen, K.H. Chen, Nano Lett. 14 (2014) 6097–6103.
[21] H.B. Zhang, J. Wei, J.C. Dong, G.G. Liu, L. Shi, P.F. An, G.X. Zhao, J.T. Kong, X.J. Wang, X.G. Meng, J. Zhang, J.H. Ye, Angew. Chem. Int. Ed. 128 (2016) 1–6.
[22] F. Dong, Q.Y. Li, Y.J. Sun, W.K. Ho, ACS Catal. 4 (2014) 4341–4350.
[23] F. Dong, Z.W. Zhao, Y.J. Sun, Y.X. Zhang, S. Yan, Z.B. Wu, Environ. Sci. Technol. 49 (2015) 12432–12440.
[24] Y.X. Gao, Y. Huang, Y. Li, Q. Zhang, J.J. Cao, W.K. Ho, S.C. Lee, ACS Sustain. Chem. Eng. 4 (2016) 6912–6920.
[25] C. Chang, L.Y. Zhu, Y. Fu, X.L. Chu, Chem. Eng. J. 233 (2013) 305–314.
[26] J.G. Yu, J.X. Low, W. Xiao, P. Zhou, M. Jaroniec, J. Am. Chem. Soc. 136 (2014) 8839–8842.
[27] J. Di, J.X. Xia, S. Yin, H. Xu, L. Xu, Y.G. Xu, M.Q. He, H.M. Li, RSC Adv. 4 (2014) 14281–14290.
[28] J.J. Sun, X.Y. Li, Q.D. Zhao, M.O. Tade, S.M. Liu, Appl. Catal. B: Environ. 219 (2017) 259–268.
[29] B.J. Liu, X.Y. Li, Q.D. Zhao, J. Ke, M. Tade, S.M. Liu, Appl. Catal. B: Environ. 185 (2016) 1–10.
[30] D.F. Xu, Y. Hai, X.C. Zhang, S.Y. Zhang, R.A. He, Appl. Surf. Sci. 400 (2017) 530–536.
[31] A. Hameed, T. Montini, V. Gombac, P. Fornasiero, J. Am. Chem. Soc. 130 (2008) 9658–9659.